remote sensing

MDPI

Article

Leaf-Level Field Spectroscopy to Discriminate Invasive Species (*Psidium guajava* L. and *Hovenia dulcis* Thunb.) from Native Tree Species in the Southern Brazilian Atlantic Forest

Caroline Lorenci Mallmann [1,2], Waterloo Pereira Filho [1], Jaqueline B. B. Dreyer [3], Luciane A. Tabaldi [4] and Flavia Machado Durgante [5,6,*]

[1] Department of Geoscience, Santa Maria Federal University, Santa Maria 97105-900, Brazil
[2] Secretary of Environment and Infrastructure for the State of Rio Grande do Sul, Porto Alegre 86010-923, Brazil
[3] Department of Forestry Engineering, Santa Maria Federal University, Santa Maria 97105-900, Brazil
[4] Department of Biology, Santa Maria Federal University, Santa Maria 97105-900, Brazil
[5] Institute of Geography and Geoecology, Karlsruhe Institute of Technology, 76131 Karlsruhe, Germany
[6] Department of Botany, National Institute for Amazonian Research, Petrópolis 69011-970, Brazil
* Correspondence: flavia.durgante@kit.edu

Abstract: Invasive species are known to have potential advantages over the native community and can be expressed in their leaf functional traits. Thus, leaf-level traits with spectral reflectance can provide valuable insights for distinguishing invasive trees from native trees in complex forest environments. We conducted field spectroscopy measurements in a subtropical area, where we also collected trait data for 12 functional traits of invasive (*Psidium guajava* and *Hovenia dulcis*), and native species (*Psidium cattleianum* and *Luehea divaricata*). We found that photosynthetic pigments were responsible for the greatest interspecific variability, especially in the green region of the spectrum at 550 nm, therefore contributing to detection of invasive species. In addition, according to LDA and stepwise procedures, the most informative reflectance spectra were concentrated in the visible range that is closely related to pigment absorption features. Furthermore, we aimed to understand the leaf optical properties of the target invasive species by using a combination of narrow bands and linear regression models. *P. guajava* showed high correlations with specific leaf area, Car/Chl and relative water content. *H. dulcis* had a strong correlation with water content, specific leaf area and Chla/Chlb. Overall, this methodology proved to be appropriate for discriminating invasive trees, although parameterization by species is necessary.

Keywords: remote sensing; invasive alien species; leaf functional traits; linear discriminant analysis; optical properties

Citation: Mallmann, C.L.; Pereira Filho, W.; Dreyer, J.B.B.; Tabaldi, L.A.; Durgante, F.M. Leaf-Level Field Spectroscopy to Discriminate Invasive Species (*Psidium guajava* L. and *Hovenia dulcis* Thunb.) from Native Tree Species in the Southern Brazilian Atlantic Forest. *Remote Sens.* **2023**, *15*, 791. https://doi.org/10.3390/rs15030791

Academic Editor: Dengsheng Lu

Received: 12 December 2022
Revised: 19 January 2023
Accepted: 20 January 2023
Published: 30 January 2023

1. Introduction

1.1. Background

From the last century onwards, plant invasions have been increasing worldwide [1,2] and have been considered a major threat to global biodiversity [3]. Invasive alien species (IAS) are introduced by humans outside of their natural range and cause negative ecological, economic, and social impacts on the novel environment [4–6]. Invasive trees are usually adaptive and competitively distinct in relation to co-occurring native species [7]. Therefore, they can alter the richness, composition and abundance of the community and also produce changes in ecosystem functioning [8].

1.2. IAS in Protected Areas

Invasive species have been reported causing risks in protected areas all over the world [9]. In Brazil, the establishment of protected areas was a main strategy for biodiversity conservation [10]. However, in addition to habitat fragmentation and the presence of

disturbed environments [11], these areas are also currently being threatened by biological invasions [12]. Outside the protected areas, land uses also need attention, as they mostly determine a strong propagule pressure and contribute to the success of plant invasions in these areas [13–17].

The occurrence of invasive species has increased in forest ecosystems in recent years, and negatively affects species composition, forest microclimate, and soil chemistry [8]. Additive or synergistic effects of habitat disturbance and species invasions, such as competition for light and nutrients, result in today's landscapes being dominated by exotic species, which is a direct consequence of this competitive exclusion [18]. Changes caused by invasive plants that disrupt ecosystem functioning and promote the invasion and establishment of new invasive plants create a feedback loop between habitat disturbance and species invasion, i.e., "invasive collapse" of disturbed ecosystems [19,20].

IAS represent an ongoing challenge for the management of protected areas associated with high economic costs [20–22]. In this regard, remote sensing can potentially contribute as a methodological approach for the detection of invasive species and their monitoring over large and hard-to-reach areas, including forests.

1.3. Leaf Optical Properties

Remote sensing (RS) in the optical domain, which can be applied to a range of environmental studies, focuses on the spectral properties of the leaf in relation to its biochemical content (chlorophyll, water, dry matter) and its anatomical structure [23]. The diffuse reflectance of a leaf, modified by its internal properties, may contain features that are useful for mapping the functional properties of leaves [24]. In a healthy green leaf, the spectral region from 430 nm to 660 nm is characterized by a strong chlorophyll a absorption peak. In contrast, the absorption range of chlorophyll b is more intense (450 nm and 650 nm). The carotenoids have an absorption peak at 450 nm. In the near infrared (NIR) region, the reflectance increases dramatically (700 nm to 1200 nm), with a reflectance peak at 900 nm. Properties extracted from leaves and their reflectance spectra are input parameters and serve to feed canopy models. Combinations of narrow bands, such as the proposition of spectral indices, consist of a classical approach in remote sensing and are widely used for extracting information related to photosynthetic pigment content, water content, and dry mass, mainly due to their simplicity, and because they usually produce good results for individual datasets [23].

1.4. Remote Sensing for the Detection, Mapping, and Monitoring of IAS

Remote sensing has been used in recent years to detect invasive plants [25–27]. IAS detection and mapping is possible due to the dominance of invasive species that can form homogeneous and large patches in the area, which contrasts the seasonal phenology of IAS and the native plants, and biochemical, physiological, or structural traits that can distinguish the IAS from the native community [28]. However, the platform and sensor used for detection must be compatible with the target species and/or the environment characteristics. Multiscale approaches, such as integrating data from different platforms and sensors, are potential methodologies for the discrimination and mapping of IAS [29–31].

Phenology-based approaches are widely used, for example, to map IAS according to flowering and leaf senescence [32–34]. On the other hand, structural traits tend to be spatially separable within a native ecosystem using processing techniques based on image segmentation. However, their application is indicated when the IAS present aggressive and dominant characteristics [35], or they form groups that are distinct from the native community [36,37].

Recent studies, such as those of Omer [38], Tesfamichael [39], and Iqbal [40], have used methods based on field spectroscopy to discriminate invasive species. Omer [38] used continuous wavelet analysis and feature reduction techniques to discriminate five invasive plant species. Tesfamichael [39] investigated the potential of remote sensing in identifying native, non-native, and hybrid *Tamarix* species in South Africa. Classification of species at

the leaf and canopy level was performed using field spectroradiometer data. Iqbal [40] used a hyperspectral field sensor to discriminate invasive plant species from adjacent native species in two protected areas in Pakistan. Spectral separability was calculated using the Jeffries-Matusita distance index based on selected wavebands.

In tropical and subtropical forest ecosystems, mapping target IAS seems to be complex as they are spread out in the woods and most have morphological traits that are similar to the native species. Therefore, methods that not only use structural traits, but also spectral data should be used [41,42]. Furthermore, to increase the potential for discrimination between native and invasive plants, physiological characteristics linked to plant functioning and growth must be included [32]. Invasive tree species can be detected directly via the forest canopy [43] or indirectly by measuring the leaves and simulating the canopy [44,45].

Functional traits at leaf-level, such as photosynthetic pigments [46], nitrogen concentration [47] and moisture content [48], are directly related to physiological functions such as photosynthesis, respiration, and transpiration. These characteristics can be reflected in the optical properties of the leaves and, when related to the spectral signatures, can contribute to improving the discrimination and mapping of IAS [49,50].

Given the importance of the topic, the present study fills a gap related to remote detection of IAS in complex forest ecosystems. Moreover, it intends to assess invasive forest species that exhibit sparse invasion characteristics and sometimes form clusters; however, these species are not characterized as monodominant. We pursued the following objectives: 1) determine leaf functional traits and spectral characterization of native and invasive trees; 2) discriminate invasive species from native species based on their reflectance values via field spectroscopy; and 3) understand the relationship between functional characteristics of invasive plants and their spectral patterns (optical types).

2. Materials and Methods

2.1. Study Site

The study was conducted at the Quarta Colonia State Park (hereafter QCSP) that protects an area of ca. 1847 ha of secondary forest in southern Brazil (29°27′57.39″ S, 53°16′51.30″ W), within the Atlantic Forest domain [51–53] (Figure 1a,c). The vegetation of QCSP is classified as seasonal deciduous and it is covered with native tree species such as *Nectandra megapotamica* (Spreng.) Mez, *Cupania vernalis* Cambess, *Trichilia clausseni* C.DC., *Chrysophyllum marginatum* (Hook. & Arn.) Radlk., *Luehea divaricata* Mart., *Sebastiania commersoniana* (Baill.) L.B.Sm. & Downs, *Allophylus edulis* (A.St.-Hil.) Hieron. ex Niederl., *Cordia americana* (L.) Gottschling & J.S.Mill. [54,55]. The landscape varies from undulating to mountainous, which leads to heterogeneous bio-physical soil conditions in which soils of the type Litolic Neosol and Regolitic Neosol predominate [56]. The mean annual temperature ranges from 18 °C to 20 °C and mean annual precipitation is approximately 1300 mm [57]. Plant invasions are a significant threat at QCSP and are closely linked to land use changes and anthropogenic impacts in the area prior to their establishment [53].

2.2. Target Species

We selected two invasive species, namely *Hovenia dulcis* Thunb. (Japanese raisin tree) and *Psidium guajava* L. (Guava), and two co-occurring native species, namely *Luehea divaricata* Mart. & Zucc. (Whips-horse) and *Psidium cattleianum* Sabine (Strawberry guava). Native–invasive species pairs were chosen according to morphological and taxonomic parameters (most similar to plant comparisons), and occurrence distribution (frequencies and population densities). (See Table S1 and Figure S1 in Supplementary Materials).

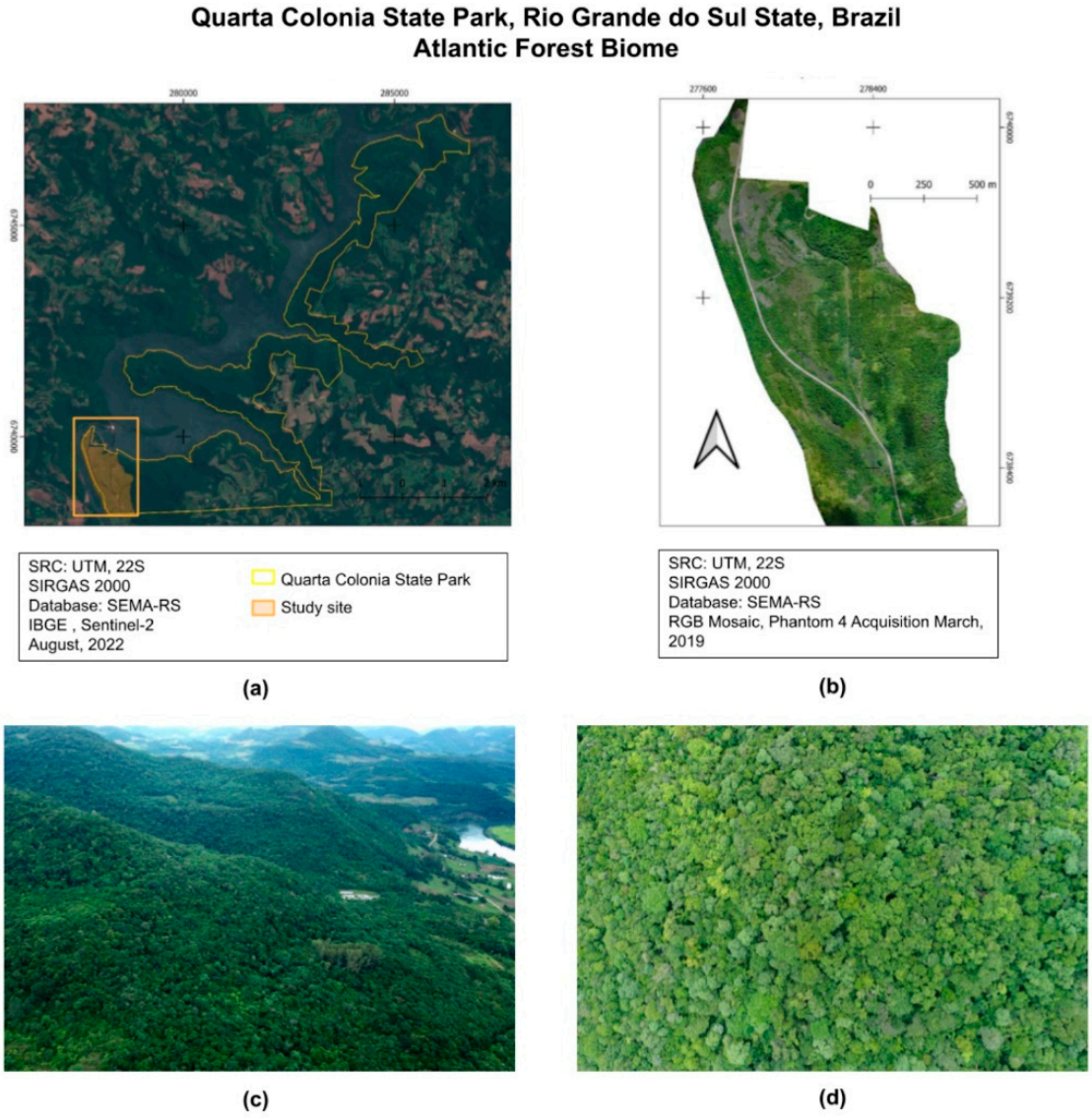

Figure 1. Images show: (**a**) Quarta Colonia State Park (QCSP); (**b**) closer view of the study site; (**c**) aerial view image of woody cover and QCSP head office; and (**d**) secondary forest canopy.

The Target IAS of the Study

Hovenia dulcis Thunberg

Hovenia dulcis, commonly known as Japanese raisin tree, is native to East Asia and grows in China, Japan, North Korea, South Korea, Thailand, and Vietnam [58]. It is described as a deciduous fast-growing tree that can reach 25 m in height, is tolerant of shade though prefers habitats with high incidences of light [59,60]. Leaves are alternate, simple, 10–15 cm long and 7–12 cm in width. It reproduces sexually by seed, and fruits are produced in large quantities [61]. It is considered to be an invasive species in forest ecosystems in South America, especially in the Atlantic Forest domain [62–64]. The species was brought to southern Brazil and introduced to rural properties motivated by economic reasons, shade and wood uses [61]. As a consequence, it has spread beyond cultivation areas and has become a growing problem in subtropical deciduous seasonal forests, often being found in the canopies of secondary forest fragments [64–66]. *H. dulcis* can outcompete other species for light and nutrients [67] and promotes changes in structure and in species composition in the plant community [68].

Psidium guajava L.

Psidium guajava (commonly known as guava) is a tropical tree from southern Mexico and northern South America that is under cultivation around the world and has become invasive in southern Brazil [69]. Adult guava trees grow to 3–8 m in height. Leaves are opposite, simple, 5–15 cm long and 3–7 cm wide [70]. It reproduces sexually and fruits are fleshy, edible, and produce large quantities of seeds [71–73]. The species is well adapted to a wide range of environmental conditions, and it can form dense monocultures and produce allelopathic effects that displace native plants [74].

2.3. Spectral Measurements in the Field

Field sampling was conducted in QCSP in the spring of 2020 when plants were actively growing and reaching greater photosynthetic capacity. The average field temperature and relative humidity were 32 °C and 49%, respectively. We collected data from six mature trees of each species. All individuals were sampled under similar solar radiation/light conditions, i.e., measurements occurred at the same time (they started at 10:00 am and ended at 1:30 pm) on cloudless and windless days in a homogeneous area with 20 years of secondary forest succession (Figure 1b,d).

Spectral data collection was conducted in three campaigns in the spring, resulting in the collection of 24 subsamples. Care was taken in the design of the sampling to represent the different light incidence directions when collecting the samples. For this purpose, six individuals (samples) per species were selected and only leaves from the upper third of the canopy were collected. The subsample was distributed among the quadrants (north, south, east, and west), with a replicate of four leaves for all variables analyzed, thus making a total of 384 measured leaves. Sampling for leaf functional traits was conducted simultaneously in the same field.

2.4. Leaf Sampling and Laboratory Processing

We analyzed 12 leaf functional traits for both native and invasive species, which were related to photosynthetic pigments, water content and vegetation structure (Table 1). These traits at leaf-level are relevant as they represent ecological strategies that can be correlated with measurable leaf spectral properties [50]. For the study, the same six individuals of each tree species previously selected were used for the measurements. In all cases, leaf sampling was conducted on the middle third of the canopy, and thirty-two healthy leaves were collected per individual. Four leaves were used in each analysis.

Table 1. Synthesis of traits and functions recorded for plant species at Quarta Colonia State Park during the 2020 field season.

Leaf Trait	Acronym	Unit	Indicator of
Water content			
Fuel moisture content	FMC	%	susceptibility of vegetation to fire
Liquid water content	LWC	%	water content estimate
Equivalent water thickness	EWT	g cm^{-2}	hydric stress
Vegetation structure			
Leaf mass per area	LMA	g cm^{-2}	leaf longevity and hardness
Specific leaf area	SLA	cm^2 g^{-1}	light capture efficiency
Photosynthetic pigments			
Chlorophyll a	Chla	µg cm^{-2}	main photosynthetic pigment
Chlorophyll b	Chlb	µg cm^{-2}	accessory pigment
Total chlorophyll	Chl	µg cm^{-2}	photosynthetic activity
Carotenoid	Car	µg cm^{-2}	photoprotective pigments
Chlorophyll a:b ratio	Chla/Chlb	-	photosynthetic response of the acclimatization process
Carotenoid:total chlorophyll ratio	Car/Chl	-	changes in development and stress photosynthetic responses
Sum of chlorophyll a and b	Chla + b	µg cm^{-2}	photosynthetic activity

To avoid the degradation of photosynthetic pigments, leaf samples were immediately wrapped in aluminum foil, frozen in liquid nitrogen, and stored on thermal box in the field until they could be transferred to a −80 °C freezer in the Plant Biotechnology Lab at Santa Maria Federal University. Fresh leaf tissues (50 mg) were then homogenized in liquid nitrogen, incubated at 65 °C with dimethyl sulfoxide (DMSO) until the pigments were completely extracted, as per Hiscox and Israelstam [75], and estimated with Lichtenthaler's formula [76]. Concentrations of chlorophyll a, chlorophyll b and carotenoids were quantified using a spectrophotometer (Spectrophotometer VM5, Celm E-205D, Bel Engineering, Monza, Italy) based on their absorbance at 663, 645 and 470 nm, respectively.

Leaf samples for water content and for structural measurements were stored in humidified bags in the field and kept in black plastic bags on thermal box to prevent wilting during transport. Leaf samples were first measured with a scanner/portable leaf area meter (Portable Leaf Area Meter -AM300, ADC BioScientific Ltd, Hoddesdon, UK) to determine the leaf area. Leaves were fresh weighed and then oven-dried at ±65 °C until constant weight before recording dry mass. We calculated leaf mass per area (LMA; g cm^{-2}) as leaf dry mass divided by leaf area. Specific leaf area (SLA; cm^2 g^{-1}) was calculated as area per unit mass.

2.5. Collection of Leaf-Level Spectral Data

For leaf spectral characterization of the target species, field spectroscopy was performed using a handheld portable spectroradiometer (ASD FieldSpec®, Malvern Panalytical, Malvern, UK) within the 300–1200 nm range, with spectral resolution of 3 nm. However, the spectral range of 400–900 nm was delimited for this work due to noise observed in the equipment. One exposed branch from the higher third of the canopy for each tree was removed and four leaves were then collected. Immediately (less than 10 min), leaf samples were overlapped and placed on a black background and leaf-level spectral reflectance signatures were recorded for each sample.

The spectroradiometer was placed vertically over the target (leaf) at a distance of 10 cm, and data was collected by 25 degrees of field of view (FOV for field measurement). The positioning of the spectroradiometer was performed by moving in constant azimuthal movement (90°). The distance between the target and the object was kept constant to ensure that no reflectance came from the surroundings of the leaf. The spectroradiometer was calibrated with a Lambertian reference plate before each sample measurement. For each target, 10 readings were collected from the reference plate and leaf sample to obtain the average spectrum. All measurements were collected with RS3 software (ASD), and ViewSpecPro software (ASD) was used for post processing of spectra files. During the field work, meteorological information, such as temperature, humidity, wind speed and solar radiation inclination associated with each individual, was also collected. A thermo hygro-anemometer and a clinometer were used.

2.6. Statistical Analyses

Our study was analyzed via the following three steps: (1) analysis of the functional traits of the native and invasive trees using leaf traits measured in the field; (2) analysis of spectral reflectance; and (3) integrated analysis of leaf functional traits and spectral reflectance (Figure 2). All the analyses were performed using Microsoft Excel (Microsoft, Redemond, Whashington, USA) and R (R Core Team 2020). A descriptive statistical analysis of all 12 traits of the target species with a 95% confidence interval (CI) is also provided. Additionally, the Kruskal–Wallis test was performed to compare the species, followed by Dunn's post hoc test.

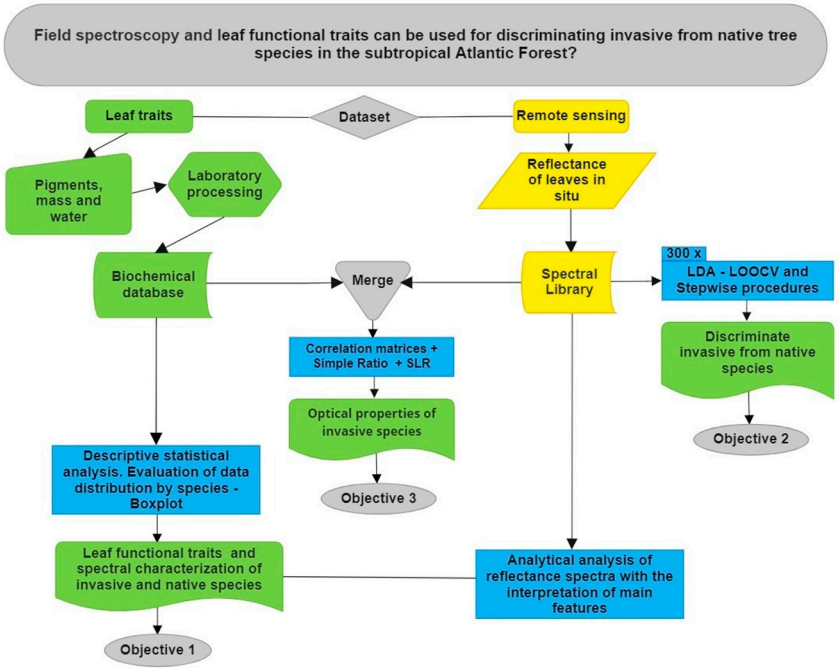

Figure 2. Schematic diagram illustrating flow of methodology. Detailed data processing and analyses are described in Section 2.6. Overall, steps represent data acquisition, data organization, processing and analysis, and results.

To evaluate the spectral signatures of the species, the analytical technique was used. Linear discriminant analysis (LDA) was performed to distinguish the spectra with two subsets; one containing 70% of the spectral data to build the model and one containing the remaining 30% of the spectral data used for validation. Then, stepwise procedures were used to select important wavelengths that best explain the differences among species. This process selects the variables one by one in accordance with the p-value < 0.05 until no variable can be entered. The leave-one-out cross-validation (LOOCV) was used to estimate the model generalization, which is a disposition of k-fold cross-validation, where k is the number of examples in the dataset (n).

To test the correlation between leaf characteristics and their respective spectral reflectance for invasive species, a simple relationship was investigated to estimate the biophysical and biochemical parameters using an interactive correlation environment (ICE) according to Ogashawara [77]. The method was adapted for Microsoft Excel and consists of a correlation matrix to select the single band ratio. First, a correlation matrix was created for each independent variable in terms of reflectance values with a resolution of 1 nm. All spectral band ratios were calculated for each variable. This procedure was performed for each of the invasive species and permitted the identification of the wavelength with the best correlation for each trait. Finally, simple linear regression (SLR) was used to determine the significant functional optical properties based on the most significant functional characteristics of the leaves according to the best simple ratio correlation (r). The performance of the models was validated using the coefficient of determination (r^2), root mean square error (RMSE), and residual sum of squares (RSS).

3. Results

3.1. Leaf Functional Traits for Native and Invasive Species

We measured twelve leaf traits that were closely related to plant photosynthesis in terms of water content, biochemical content, and leaf structure and physiology based on dry mass. The statistical summary of the analyses can be found in the Supplementary Materials (see Table S2 in Supplementary Materials).

3.1.1. Water Content

In general, the water content differed between species according to the Kruskal–Wallis test (Table 2). However, after post hoc testing, the significant differences were found for the EWT trait (Table 3). The native species *L. divaricata* had the highest LWC for the total dataset and the highest intraspecific variability. Nonetheless, when comparing the means, the invasive *H. dulcis* presented the highest mean value among the species (Figure 3a). The native species showed greater FMC as well as greater intraspecific variability. In contrast, invasive species had lower values for data amplitude and lower intraspecific variability (Figure 3b). The results also showed that, in general, both invasive species presented lower EWT values when compared to the corresponding native species, and less intraspecific variability (Figure 3c).

Table 2. Kruskal–Wallis rank-sum test of the 3 leaf traits Water content: LWC (%) = liquid water content; FMC (%) = fuel moisture content; EWT (g cm^{-2}) = equivalent water thickness; significance ($p \leq 0.05$).

	chi-Squared	**df**	***p*-Value**
LWC	10.747	3	0.01318
FMC	10.747	3	0.01318
EWT	53.874	3	1.19×10^{-8}

Table 3. Dunn's post hoc test adjusted using the *Bonferroni* method for the three leaf traits. Water content: LWC (%) = liquid water content; FMC (%) = fuel moisture content; EWT (g cm^{-2}) = equivalent water thickness for 24 subsamples collected from each species invasive (PG = *Psidium guajava* an HD= *Hovenia* dulcis) and native (PC= *Psidium cattleianum* and LD= *Luehea divaricata*).

Trait	**Species Group_**		**Statistic**	***p*-Value**	**p.Adjust**
LWC	HD	LD	−2.34	0.0194	0.117
	HD	PC	−2.09	0.0368	0.221
	HD	PG	−3.14	0.00169	0.0101
	LD	PC	0.249	0.804	1
	LD	PG	−0.803	0.422	1
	PC	PG	−1.05	0.293	1
FMC	HD	LD	−2.34	0.0194	0.117
	HD	PC	−2.09	0.0368	0.221
	HD	PG	−3.14	0.00169	0.0101
	LD	PC	0.249	0.804	1
	LD	PG	−0.803	0.422	1
	PC	PG	−1.05	0.293	1
EWT	HD	LD	1.29	1.97×10^{-11}	0
	HD	PC	6.84	7.67×10^{-12}	4.60×10^{-11}
	HD	PG	3.51	4.43×10^{-4}	2.66×10^{-3}
	LD	PC	5.55	2.78×10^{-8}	1.67×10^{-7}
	LD	PG	2.22	2.62×10^{-2}	1.57×10^{-1}
	PC	PG	−3.33	8.63×10^{-4}	5.18×10^{-3}

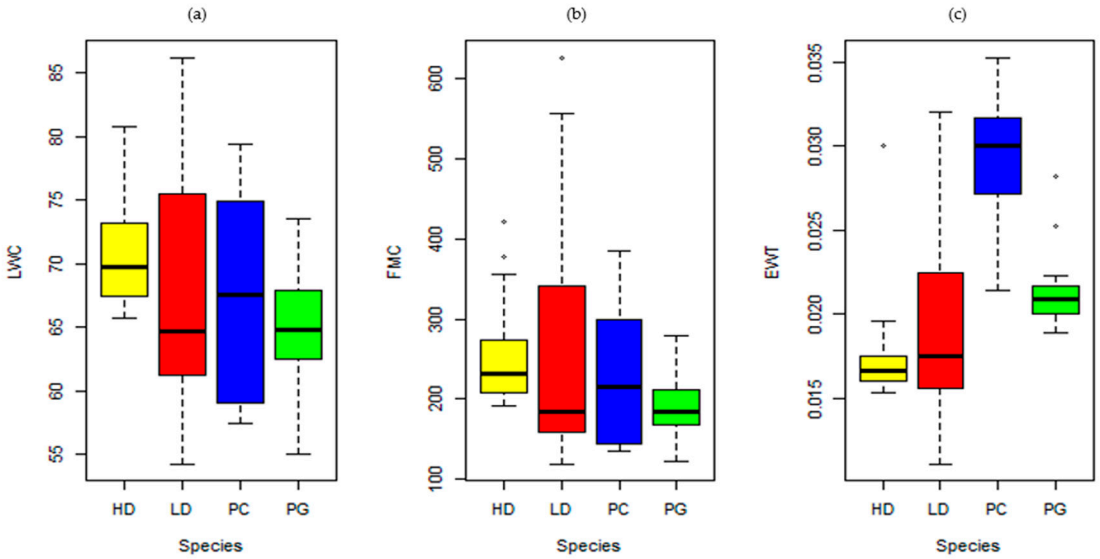

Figure 3. Boxplot of leaf-level functional traits. Water content: (**a**) LWC (%) = liquid water content; (**b**) FMC (%) = fuel moisture content; and (**c**) EWT (g cm^{-2}) = equivalent water thickness; were the species are: HD (yellow) = *Hovenia dulcis*; LD (red) = *Luehea divaricata*; PC (blue) = *Psidium cattleianum*; PG (green) = *Psidium guajava*. * Indicates outliers.

3.1.2. Vegetation Structure

The traits related to vegetation structure showed significant difference between species (Table 4). After the post hoc test (Table 5), the greatest differences were observed among the groups: invasive species *H. dulcis* and *P. guajava*; invasive species *H. dulcis* and native *P. cattleianum*; followed by the native species *L. divaricata* and *P. cattleinum*.

Table 4. Kruskal–Wallis rank-sum test of the two leaf traits Vegetation structure: LMA (g cm^{-2}) = leaf mass per area; SLA (cm^2 g^{-1}) = specific leaf area; significance ($p \leq 0.05$).

	chi-Squared	df	*p*-Value
LMA	46.129	3	5.33×10^{-7}
SLA	46.554	3	4.32×10^{-7}

Table 5. Dunn's post hoc test adjusted using the *Bonferroni* method for the two leaf traits. Vegetation structure: LMA (g cm^{-2}) = leaf mass per area; SLA (cm^2 g^{-1}) = specific leaf area for 24 subsamples collected from each invasive species (PG = *Psidium guajava* and HD = *Hovenia dulcis*) and native species (PC = *Psidium cattleianum* and LD = *Luehea divaricata*).

Trait	Species Group_		Statistic	*p*-Value	p.Adjust
LMA	HD	LD	1.86	0.0622	0.373
	HD	PC	6.01	1.81×10^{-9}	1.08×10^{-8}
	HD	PG	4.97	6.79×10^{-7}	4.08×10^{-6}
	LD	PC	4.15	3.34×10^{-5}	2.00×10^{-4}
	LD	PG	3.10	0.00192	0.0115
	PC	PG	1.05	0.295	1
SLA	HD	LD	−1.99	0.0461	0.260
	HD	PC	−6.04	1.58×10^{-9}	9.46×10^{-9}
	HD	PG	−5.09	3.62×10^{-7}	2.17×10^{-6}
	LD	PC	−4.04	5.31×10^{-5}	3.19×10^{-4}
	LD	PG	−3.09	0.00198	0.0119
	PC	PG	0.948	0.343	1

The evergreen species (*P. cattleianum* and *P. guajava*) in this study showed greater leaf mass per area (LMA; Figure 4a). On the other hand, the deciduous species (*L. divaricata* and *H. dulcis*) exhibited higher values of specific leaf area (SLA; Figure 4b). The native *Psidium cattleianum* presented the highest LMA (LMA = 0.018 g cm^{-2}) and the smallest SLA (SLA = 40.56 cm^2 g^{-1}). In contrast, the invasive *Hovenia dulcis* had the lowest LMA (LMA = 0.004 g cm^{-2}) and the largest SLA (SLA = 225.32 cm^2 g^{-1}).

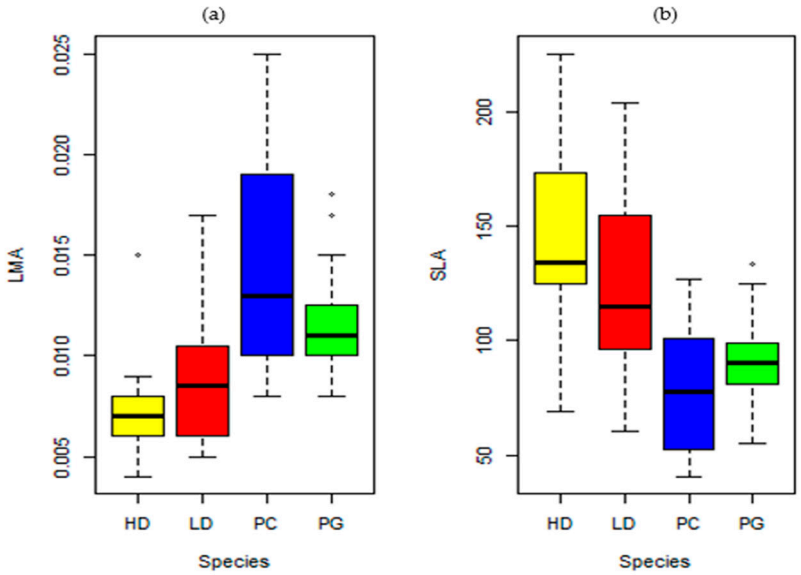

Figure 4. Boxplot of leaf-level functional traits. Vegetation structure: (**a**) LMA (g cm^{-2}) = leaf mass per area; (**b**) SLA (cm^2 g^{-1}) = specific leaf area; where the species are HD (yellow) = *Hovenia dulcis*; LD (red) = *Luehea divaricata*; PC (blue) = *Psidium cattleianum*; PG (green) = *Psidium guajava*. * Indicates outliers.

3.1.3. Photosynthetic Pigments

Photosynthetic pigments showed significant differences among the analyzed species groups, except for Car/Chl (Table 6). After the post hoc test, the differences found between the groups of corresponding invasive and native species, *H. dulcis* × *L. divaricata* and *P. guajava* × *P. cattleianum*, for the traits: Chla, Chlb, Chltotal, Car (Table 7).

Table 6. Kruskal–Wallis rank-sum test of the seven leaf traits. Photosynthetic pigments: Chla (μg cm^{-2}) = chlorophyll a content; Chlb (μg cm^{-2}) = chlorophyll b content; Chl (μg cm^{-2}) = total chlorophyll content; Car (μg cm^{-2}) = carotenoid content; Chla/Chlb = chlorophyll a:b ratio; Car/Chl = carotenoid: total chlorophyll ratio; Chla + b = sum of chlorophyll a and b; significance ($p \leq 0.05$).

	chi-Squared	**df**	***p*-Value**
Chla	37.419	3	3.75×10^{-5}
Chlb	24.978	3	1.56×10^{-2}
Chltotal	33.853	3	2.13×10^{-4}
Car	39.859	3	1.14×10^{-5}
Chla/Chlb	36.271	3	6.56×10^{-5}
Car/Chl	51.107	3	0.1639
Chla + b	34.322	3	1.70×10^{-4}

Table 7. Dunn *post hoc* test by the adjusted method *Bonferroni* of the 7 leaf traits Photosynthetic pigments: Chla (μg cm^{-2}) = chlorophyll a content; Chlb (μg cm^{-2}) = chlorophyll b content; Chl (μg cm^{-2}) = total chlorophyll content; Car (μg cm^{-2}) = carotenoid content; Chla/Chlb = chlorophyll a:b ratio; Car/Chl = carotenoid:total chlorophyll ratio; Chla + b = sum of chlorophyll a and b for 24 subsamples collected from each species invasive (PG = *Psidium guajava* an HD= *Hovenia dulcis*) and native (PC= *Psidium cattleianum* and LD= *Luehea divaricate*).

Trait	Group_Species		Statistic	*p*-Value	p.Adjust
Chla	HD	LD	2.94	0.00325	0.0195
	HD	PC	−2.68	0.00728	0.0437
	HD	PG	2.04	0.0412	0.247
	LD	PC	−5.63	1.83×10^{-8}	1.10×10^{-7}
	LD	PG	−0.902	0.367	1
	PC	PG	4.73	2.30×10^{-6}	1.38×10^{-5}
Chlb	HD	LD	3.28	1.34×10^{-4}	8.05×10^{-4}
	HD	PC	0.663	0.507	1
	HD	PG	3.85	1.18×10^{-4}	7.09×10^{-4}
	LD	PC	−3.16	0.00160	0.00961
	LD	PG	0.0311	0.975	1
	PC	PG	3.19	0.00144	0.00864
Chltotal	HD	LD	3.34	0.000603	0.00362
	HD	PC	−1.63	0.103	0.616
	HD	PG	2.78	0.00540	0.0324
	LD	PC	−5.06	4.14×10^{-7}	2.49×10^{-6}
	LD	PG	−0.648	0.517	1
	PC	PG	4.41	1.01×10^{-5}	6.07×10^{-5}
Car	HD	LD	3.63	0.000287	0.00172
	HD	PC	−1.29	0.197	1
	HD	PG	3.82	0.000134	0.000805
	LD	PC	−4.92	8.78×10^{-7}	5.27×10^{-6}
	LD	PG	0.192	0.848	1
	PC	PG	5.11	3.24×10^{-7}	1.94×10^{-6}
Chla/Chlb	HD	LD	−2.27	0.229	0.138
	HD	PC	−5.63	1.78×10^{-8}	1.07×10^{-7}
	HD	PG	−4.30	1.70×10^{-5}	1.02×10^{-4}
	LD	PC	−3.36	0.000786	0.00472
	LD	PG	−2.03	0.0428	0.257
	PC	PG	1.33	0.183	1
Car/Chl	HD	LD	−2.27	0.229	0.138
	HD	PC	−5.63	1.78×10^{-8}	1.07×10^{-7}
	HD	PG	−4.30	1.70×10^{-5}	1.02×10^{-4}
	LD	PC	−3.36	0.000786	0.00472
	LD	PG	−2.03	0.0428	0.257
	PC	PG	1.33	0.183	1
Chla + b	HD	LD	3.39	0.000702	0.00421
	HD	PC	−1.74	0.0817	0.490
	HD	PG	2.73	0.00642	0.0385
	LD	PC	−5.13	2.90×10^{-7}	1.74×10^{-6}
	LD	PG	−0.663	0.507	1
	PC	PG	4.47	7.96×10^{-6}	4.77×10^{-5}

For leaf chlorophyll a content (23.75 ± 8.98 μg cm^{-2}), high values were indicated for *L. divaricata* (Chla = 30.38 μg cm^{-2}) and *P. guajava* (Chla = 25.96 μg cm^{-2}), then for *H. dulcis* (21.45 μg cm^{-2}) and *P. cattleianum* (15.55 μg cm^{-2}; Figure 5a). For chlo-rophyll b, high contents were also observed for *L. divaricata* (Chlb = 9.46 μg cm^{-2}) and *P. guajava* (Chlb = 8.88 μg cm^{-2}), followed by *P. cattleianum* (Chlb = 6.42 μg cm^{-2}) and *H. dulcis* (Chlb = 5.9 μg cm^{-2}; Figure 5b). Again, *L. divaricata* (Chl = 115.3 μg cm^{-2}; Chl a + b = 63.8 μg cm^{-2}) and *P.*

guajava (Chl = 103.8 μg cm^{-2}; Chl a + b = 57.4 μg cm^{-2}) showed greater Chl and Chl a + b contents (Figures 5c and 6c). In general, IAS presented less intraspecific variability, on average, than native species.

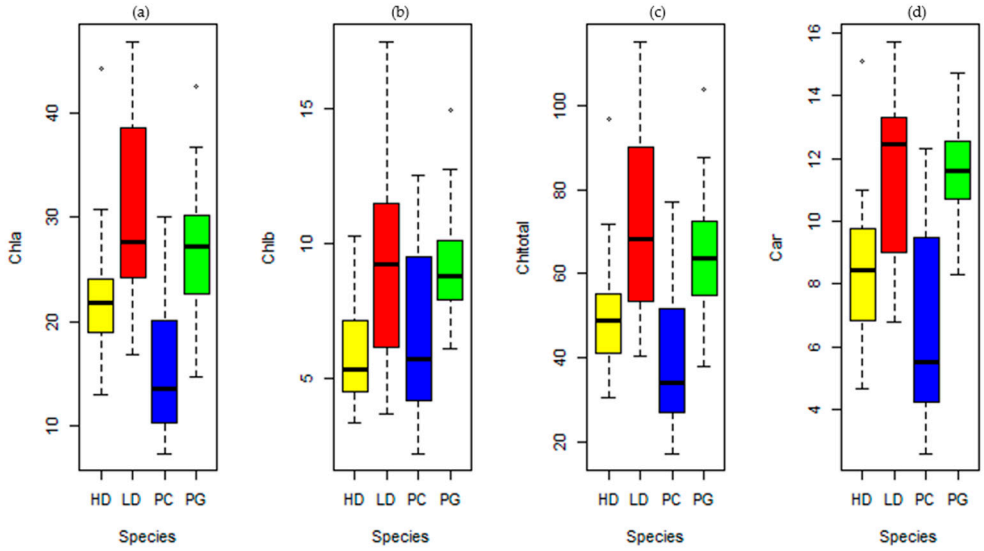

Figure 5. Boxplot of leaf-level functional traits Photosynthetic pigments: (**a**) Chla (μg cm^{-2}) = chlorophyll a content; (**b**) Chlb (μg cm^{-2}) = chlorophyll b content; (**c**) Chl (μg cm^{-2}) = total chlorophyll content; and (**d**) Car (μg cm^{-2}) = carotenoid content; where the species are:HD (yellow) = *Hovenia dulcis*; LD (red)= *Luehea divaricata*; PC (blue) = *Psidium cattleianum*; PG (green)= *Psidium guajava*. * Indicates outliers.

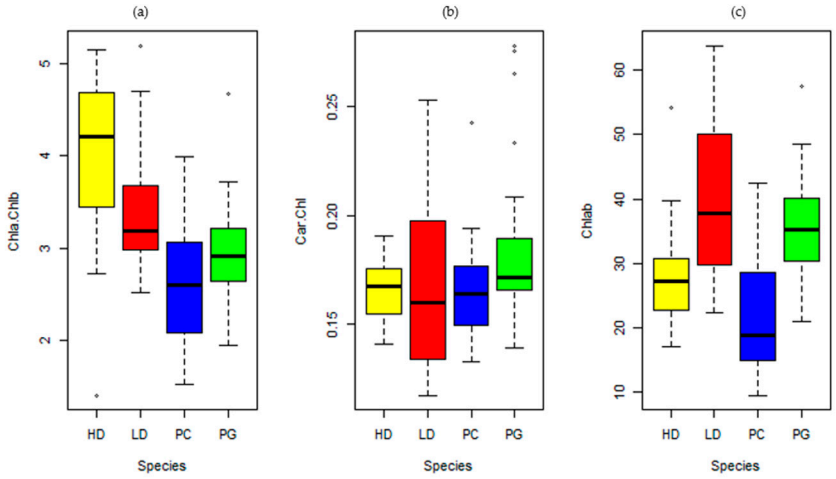

Figure 6. Boxplot of leaf-level functional traits. Photosynthetic pigments: (**a**) Chla/Chlb = chlorophyll a:b ratio; (**b**) Car/Chl = carotenoid:total chlorophyll ratio; (**c**) Chla + b = sum of chlorophyll a and b; were the species are: HD (yellow) = *Hovenia dulcis*; LD (red)= *Luehea divaricata*; PC (blue) = *Psidium cattleianum*; PG (green)= *Psidium guajava*. * Indicates outliers.

The lowest Chla/Chlb rates were associated with the *Psidium* congeneric species, such as *P. cattleianum* (Chla/Chlb = 2.58) and *P. guajava* (Chla/Chlb = 2.85; Figure 6a). Our results showed that although these species are described as initial secondary, in general, they could present shade-tolerant behavior. This suggests that *P. guajava* is also capable of extending the range of invasion from degraded areas and forest edges, where it usually occurs, to the understory of subtropical forests and, consequently, this should alert land managers to the risk. In contrast, *H. dulcis* showed the highest Chla/Chlb rates (Chla/Chlb = 2.58). This

was expected as this IAS is associated with light demand characteristics, and, therefore, its invasion process is favored by the degradation and disturbance of forest ecosystems

Generally, leaf carotenoid content is found in the same proportion as chlorophyll a in the PSI and PSII photosystems. However, we found carotenoids to be around 2.5 times more abundant than Chl a. The highest contents were described for *L. divaricata* (Car = 11.49 μg cm^{-2}) and *P. guajava*, which also had the highest Car/Chl ratio (Car = 11.59 μg cm^{-2}; Car/Chl = 0.18; Figures 5d and 6b).

3.2. Leaf Spectral Reflectance

Differences in the spectral feature of species occur mainly in magnitude, as observed for the species shown here in Figure 7a. Two spectral regions showed a greater difference in features between species, the region of the spectral domain of green and NIR. In the green range, a gradual increase was observed for all species (Figure 7b), which was even higher for the invasive species. Furthermore, there was an approximation between the native species (*P. cattleianum* and *L. divaricata*) and, consequently, a greater distance in terms of magnitude, compared to the invasive species (*P. guajava* and *H. dulcis*). Results also showed that, in general, the NIR region of the spectrum was able to distinguish the invasive species with deciduous characteristics. The highest reflectance values were for the invasive *H. dulcis* (55%) when compared to the native *L. divaricata* (45%; Figure 7c).

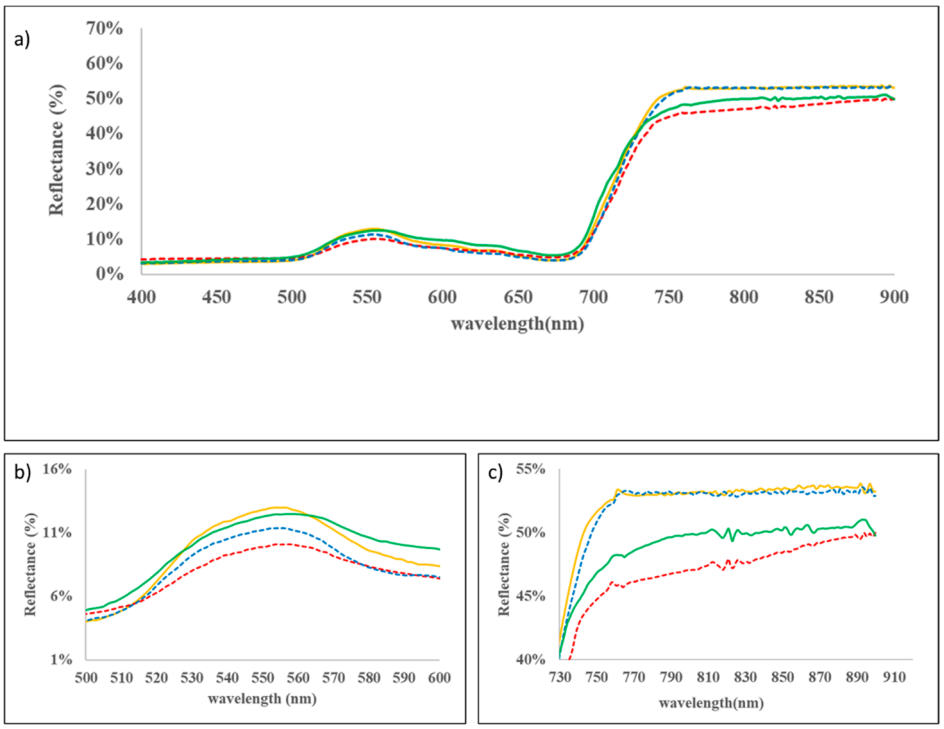

Figure 7. Leaf-level spectral reflectance curves of the four target species: *Psidium cattleianum* (blue), *Psidium guajava* (green), *Luehea divaricata* (red) and *Hovenia dulcis* (yellow) with spectral ranges at 400–900 nm (**a**); zoom in green spectral range (**b**); and zoom in NIR spectral range (**c**). Native species are represented by the dashed lines, and invasive species by the solid lines.

3.3. Discrimination of Reflectance Spectra

For the discrimination between native and invasive species, the model created using LDA achieved an overall accuracy of 97% via the 70/30 method, which indicates accurate discrimination. While LD1 clearly separated the native *L. divaricata*, LD2 was effective for the invasive *H. dulcis*. For the discrimination of the invasive *P. guajava* and the native *P. cattleianum*, the combination of the first and second discriminants was necessary (Figure 8).

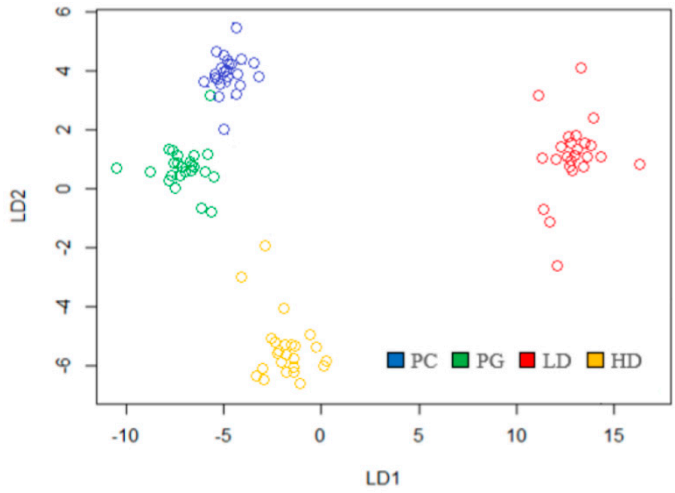

Figure 8. Two-dimensional linear discriminant analysis (LDA) of leaf reflectance for the four target species. PC (blue) = *Psidium cattleianum*; PG (green) = *Psidium guajava*; LD (red) = *Luehea divaricata*; HD (yellow) = *Hovenia dulcis*.

The confusion matrix of the best-performing LDA model (Table 8) demonstrates the ability of generalization for the total set of samples, which achieved 95% classification accuracy.

Table 8. Confusion matrix obtained from the LDA-LOOCV species classification model showing invasive and native species. Numbers in the diagonal of the matrix are the number of samples predicted correctly. Were: *P. cattleianum- Psidium cattleianum*; *P.guajava- Psidium guajava; H. dulcis- Hovenia dulcis*; *L. divaricata- Luehea divaricata*.

	P. cattleianum	*P. guajava*	*H. dulcis*	*L.divaricata*	n
P. cattleianum	**21**	1	2		24
P. guajava	2	**22**			24
H. dulcis			**24**		24
L. divaricata	2	1		**21**	24

The stepwise method was applied to identify the most informative variables that contributed to distinguishing IAS from native species. Thus, 32 spectral bands from the visible range were selected as the most significant for discriminating the species in this study (Table 9). Moreover, these bands are where pigment absorption features can be detected.

Table 9. Most-significant spectral bands selected by stepwise procedures. Blue, green and red are the wavelength regions.

Blue	Green	Red
403–407	503–504	614
467	516	668
484	532–535	694–696
497	545–548	705
	553	711
	561–564	
	579–580	
	585	
	589–592	

3.4. Leaf Optical Properties of the Invasive Target Species

The most significant simple ratio (SR) was individually selected for each leaf trait of each IAS. The most-significant optical properties for each group of leaf traits (water content, vegetation structure and photosynthetic pigments) are shown in in Table 10 and Figure 9. The total set of leaf traits analyzed, and their respective SR can be found in the Supplementary Materials (see Tables S2 and S3, and Figures S2 and S3).

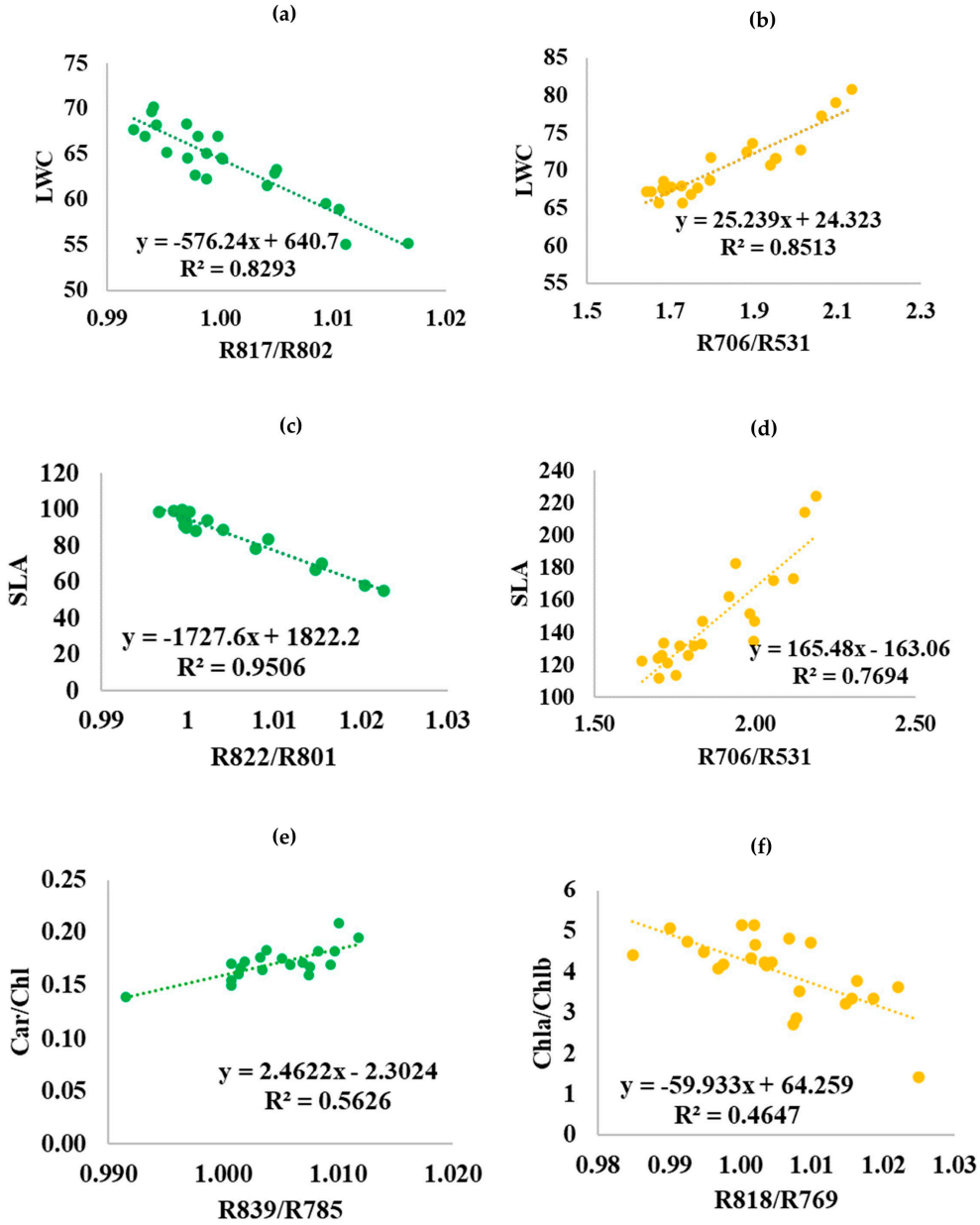

Figure 9. Simple linear regression (SLR) for the most-significant functional optical properties and simple ratios (SR). Regressions are performed for the target invasive species *Psidium guajava* (PG, green = (**a**–**c**)) and Hovenia dulcis (HD, yellow = (**d**–**f**)). Substitute to (PG, green = (**a**,**c** and **e**)) and Hovenia dulcis (HD, yellow = (**d**, **e** and **f**)).

Table 10. Summary of the most-significant leaf optical properties and leaf characteristics of two invasive tree species in QCSP. LWC (%) = liquid water content; SLA ($cm^2.g^{-1}$) = specific leaf area; Chla/Chlb = chlorophyll a:b ratio; Car/Chl = carotenoid:total chlorophyll ratio; SR= simple ratio, n = number of samples, r = simple ratio correlation; r^2 = coefficient of determination; RMSE = root mean square error; CV = coefficient of variation; RSS = residual sum of squares. Significant results at $\alpha = 0.01$, and at a 99% confidence level (p-value < 0.01).

Traits	SR	n	Mean	r	r^2	RMSE	CV%	RSS
Psidium guajava								
LWC	R817/R802	22	64.125	0.91	0.83	1.76	0.027	62.55
SLA	R822/R801	18	85.89	0.97	0.95	3.20	0.037	172.2
Car/Chl	R839/R785	20	0.171	0.75	0.56	0.01	0.061	0.002
Hovenia dulcis								
LWC	R706/R531	22	70.4	0.92	0.85	1.67	0.02	56.2
SLA	R706/R531	21	147	0.88	0.77	15.4	0.10	488
Chla/Chlb	R818/R769	23	4.0	0.7	0.47	0.66	0.16	9.6

According to the simple linear regression (Figure 9), *P. guajava* expressed the strongest correlations in NIR. The NIR reflectance ratio between 817 and 802 nm was correlated with LWC (r = 0.91), thus it was one of the best bands to predict the water content in *P. guajava* leaves (Figure 9a). However, we know that this result may not be exclusively related to water content. For SLA, a narrow waveband of NIR (R822/R801) showed good accuracy (r^2 = 0.95) (Figure 9c). For Car/Chl, the spectral behavior of the species suggests an increase in reflectance at 839 nm and 785 nm) (r = 0.75), and an increase in carotenoids in leaves at the same time (Figure 9e).

Additionally, the other invasive species, *H. dulcis,* showed a strong correlation with LWC (r = 0.92) and SLA (r = 0.88) at the same reflectance ratio (R706/R532) in the visible region of the spectrum (Figure 9b,d). Lastly, Chla/Chlb was best correlated with R818 (NIR) and R769 (red) (Figure 9f). Analyzing the increase in reflectance in NIR, we can relate it to a decrease in chlorophyll a content and, consequently, an increase in chlorophyll b.

4. Discussion

The detection and mapping of IAS still represents a major challenge in remote sensing, especially in complex forest ecosystems [42,78]. Tropical and subtropical forests, mainly in the Atlantic Forest domain, still have not been studied in depth [79]. In this paper, the use of field spectrometry for native and invasive tree species discrimination was developed based on leaf functional traits and proved to be appropriate.

4.1. Characterization of Leaf Functional Traits and Spectral Behavior

The optical properties of leaves are related to their biochemical composition and structure depending on the species and the phenological age of the leaves [28]. Considering that the spectral curves of green leaves are generally similar in shape, the difference is mainly in magnitude, as was observed for the species in our study. The optical properties of water are well known [80], and EWT and FMC are two different ways to define leaf water content. As described by [81], these two attributes are perfectly correlated when LMA is constant. However, this was not observed since LMA was not constant for our species. In general, IAS presented lower FWC, FMC and EWT when compared to the native species. Mainly, low FMC values may suggest that invasive species are more susceptible to fire at leaf and canopy levels, thus increasing the risk of wildfires in invaded areas [80–83].

Leaf reflectance proved successful for generating LMA and SLA estimates [84]. However, there appears to be little agreement between physical and empirical bases of the methods, beyond which spectral wavelengths fit best for estimation [85]. Quantitative information on LMA provides a better understanding of the taxonomy of functional groups,

regulation of physiological mechanisms and ecosystem functioning [86–88]. On the other hand, SLA is considered one of the main functional traits that drive plant differentiation since it is directly related to the efficiency of water use and, therefore, consists of a variable potential for the spectral characterization of vegetation [89–93]. Overall, deciduous species showed higher SLA than evergreen species; however, when the species were classified based on their origins, the IAS had higher SLA values, thus summarizing ecological strategies such as those related to the acquisitive end of the leaf economic spectrum and faster growing species [94]. The values obtained for LMA in this study confirm what was described by [28], i.e., that deciduous species are associated with lower LMA (*H. dulcis* and *L. divaricata*) when compared to evergreen species (*P. guajava* and *P. cattleianum*).

Photosynthetic pigments indicate that there is potential to differentiate species [80]. A marked difference was noticed in the green region at 550 nm, as mentioned by [95]. Additionally, the near-infrared reflectance plateau at 850 nm indicates the wavelength region with the greatest reflectance as well as the greatest differences between species [28]. The red edge, around 750 nm, demonstrates a distinct reflectance peak between the co-competing invasive and native species (*H. dulcis* × *L. divaricata* and *P. guajava* × *P. cattleianum*).

4.2. Spectral Discrimination of IAS from Native Species

Our results show that the VIS wavelengths are an important spectral region for discriminating the species, especially for pigment absorption features [28,96,97]. Moreover, differences in pigment content in the visible range are detected when comparing invasive and native species at the same site. [40] discriminated more plant species pairs (invasive species from the native species) within VIS regions (84%) than in NIR regions (60%). Our study also confirms the limitations of NIR as mentioned by [98] for 26 tree species in a tropical dry forest in Costa Rica. The reflectance in NIR has shown to be more promising for differentiating tree functional types based on leaf phenology (evergreen and deciduous species) than for differentiating IAS from the native community.

4.3. Leaf Optical Properties of IAS

Understanding the relationship between leaf functional traits and optical types of plants is still a knowledge gap [99]. Thus, we sought to fill this gap mainly on IAS in this study. *Psidium guajava* expressed the strongest correlations for LWC and SLA in NIR. Previous studies also proposed models based on wavelengths located in the NIR region for SLA [87,100] and for LWC [101]. Carotenoid and Car/Chl ratio contents represent indicators of photosynthetic activity and photoprotective mechanisms in plants [97]. Recently, [102] proposed two models exclusively in the VIS region (500, 660 and 700 nm) and accurately described Car/Chl changes in the range from 0.15 (r^2 = 0.87) to 0.6 (r^2 = 0.82), requiring no species-specific parameterization. Although the response obtained in our study may suggest the activation of photoprotection mechanisms by the species [97]. *Hovenia dulcis*, however, was optically significant for LWC and SLA in a narrow waveband of the visible region (R706/R530). Additionally, we found that the species seems to be water-efficient, even though water absorption is low in this region [103], and high correlations may be associated with leaf chlorophyll content [104] and structural aspects [28]. Even so, we must consider that the species did not have excessive losses in terms of water content, and the increase in visible reflectance reflects the increase in liquid water content.

5. Conclusions

It was shown that field spectroscopy is a potential method for correct discrimination of IAS from their co-occurring native species in the subtropical Brazilian Atlantic Forest. Although this method requires target species parameterization, these results are consistent, and the technique may be extended to other IAS and sites within the same subtropical forest ecosystem. This study is also important for the development of Dossel models with the goal of increasing the space–time resolution, and can be used with airborne or space-based remote sensing. We emphasize the importance of adding species leaf traits to

the spectral database, as this may advance the expansion of knowledge in the field. Finally, the outcomes observed in this study may contribute to monitoring and improving IAS control practices in protected areas.

From this study we can conclude that:

1. Linear discriminant analysis (LDA) can be used to accurately discriminate *Psidium guajava* and *Hovenia dulcis* from *Psidium cattleianum* and *Luehea divaricata*;
2. The greatest discrimination for IAS is located in the VIS region, specifically in the red (705 nm) and green regions (553 nm), which are known for being highly sensitive to pigment content variation. This suggests improved separability in chlorophyll absorption pits, as it also may suggest that the difference in anthocyanin content may enhance discrimination between species;
3. For both IAS, the LWC and SLA showed similar behavior;
4. *P. guajava* correlated to Car/Chl (R = 0.75) in NIR (R839/R785), which may suggest photoprotection activation. This provides an efficient process of acclimatization to environments normally unfavorable for other species;
5. *H. dulcis* was best correlated to Chla/Chlb at R818/R769 (R = 0.7), which may suggest that photosynthetic activity is maintained even under conditions of high luminosity and temperature;
6. IAS showed good correlation with Car/Clh and Chla/Chlb. Therefore, we may extend the space-time resolution based on data from orbital and suborbital platforms.

Supplementary Materials: The following are available online at https://www.mdpi.com/article/10.3390/rs15030791/s1, Figure S1. Native-invasive species pairs according to tree functional types based on leaf phenology (columns: evergreen and deciduous species), and origin occurrence (lines: native and invasive species). Images were obtained by scanning the leaves in the laboratory. Figure S2. Simple linear regression (SLR) for the most significant functional optical properties and simple ratios (SR). Regressions are performed for the target invasive species *Psidium guajava* (PG). Water content: (a) FMC (%) = Fuel moisture content; (b) EWT (g cm^{-2}) = Equivalent water thickness; Vegetation structure: (c) LMA (g cm^{-2}) = Leaf mass area; Photosynthetic pigments (d) Chl (µg cm^{-2}) = Total chlorophyll, (e) Chla+b (µg cm^{-2}) = Sum of chlorophyll a and b, (f) Chla (µg cm^{-2}) = Chlorophyll a, (g) Chlb (µg cm^{-2})= Chlorophyll b, (h) Car (µg cm^{-2}) = Carotenoid,(i) Chla/Chlb = Chlorophyll a:b ratio. Significant results at $\alpha = 0.01$, and at a 99% confidence level (p-value < 0.01). Figure S3. Simple linear regression (SLR) for the most significant functional optical properties and simple ratios (SR). Regressions are performed for the target invasive species *Hovenia dulcis* (HD). Water content: (a) FMC (%) = Fuel moisture content; (b) EWT (g cm^{-2}) = Equivalent water thickness; Vegetation structure: (c) LMA (g cm^{-2}) = Leaf mass area; Photosynthetic pigments: (d) Chl (µg cm^{-2}) = Total chlorophyll, (e) Chla+b (µg cm^{-2}) = Sum of chlorophyll a and b, (f) Chla (µg cm^{-2}) = Chlorophyll a,(g) Chlb (µg cm^{-2}) = Chlorophyll b, (h) Car (µg cm^{-2}) = Carotenoid, (i) Car/Chl = Carotenoid: total chlorophyll ratio. Significant results at $\alpha = 0.01$, and at a 99% confidence level (p-value < 0.01). Table S1. Comparative table of study target species (native x invasive) with key taxonomic, morphological, biological and ecological characteristics. Table S2. Summary of statistical analysis of 12 leaf traits for 96 subsamples collected from the four target species, namely *P. cattleianum*, *P. guajava*, *L. divaricata* and *H. dulcis*. FMC (%) = fuel moisture content; LWC (%) = liquid water content; EWT (g cm^{-2}) = equivalent water thickness; LMA (g cm^{-2}) = leaf mass per area; SLA (cm^2 g^{-1}) = specific leaf area; Chla (µg cm^{-2}) = chlorophyll a content; Chlb (µg cm^{-2}) = chlorophyll b content; Chl (µg cm^{-2}) = total chlorophyll content; Car (µg cm^{-2}) = carotenoid content; Chla/Chlb = chlorophyll a:b ratio; Car/Chl = carotenoid: total chlorophyll ratio; Chla+b = sum of chlorophyll a and b. Significant results at $\alpha = 0.05$. Table S3. Summary of the other leaf characteristics of Psidium guajava and the respective most significative simple ratio (SR); n = number of samples, r = simple ratio correlation; r^2 = coefficient of determination; RMSR = root mean square error; CV = coefficient of variation; RSS = residual sum of squares. Significant results at $\alpha = 0.01$, and at a 99% confidence level (p-value < 0.01). Table S4. Summary of the other leaf characteristics of Hovenia dulcis and its respective most significative simple ratio (SR); n = number of samples, r = simple ratio correlation; r^2 = coefficient of determination; RMSR = root mean square error; CV = coefficient of variation; RSS = residual sum of squares. Significant results at $\alpha = 0.01$, and at a 99% confidence level (p-value < 0.01).

Author Contributions: Conceptualization, C.L.M. and W.P.F.; methodology, C.L.M., W.P.F., J.B.B.D., L.A.T. and F.M.D.; formal analysis, C.L.M. and F.M.D.; resources, C.L.M., W.P.F., L.A.T. and F.M.D.; writing—original draft preparation, C.L.M. and J.B.B.D.; writing—review and editing, C.L.M., W.P.F., J.B.B.D., L.A.T. and F.M.D.; supervision, C.L.M.; project administration, W.P.F. All authors have read and agreed to the published version of the manuscript.

Funding: This research received no external funding.

Institutional Review Board Statement: Not applicable.

Informed Consent Statement: Not applicable.

Data Availability Statement: The data presented in this study are available on request from the corresponding author.

Acknowledgments: We would like to thank the Secretary of Environment and Infrastructure of Rio Grande do Sul—Brazil, in particular the entire team of the Quarta Colonia State Park. Thanks are also due to post-graduate course in Geography at the Federal University of Santa Maria, Brazil. As part of the ATTO project, FD acknowledges support from the German Federal Ministry of Education and Research (BMBF contracts 01LK1602F and 01LK2102D), as well as support from the KIT-Publication Fund of the Karlsruhe Institute of Technology.

Conflicts of Interest: The authors declare that there are no conflict of interest.

References

1. Seebens, H.; Blackburn, T.; Dyer, E. No saturation in the accumulation of alien species worldwide. *Nat. Commun.* **2017**, *8*, 14435. [CrossRef] [PubMed]
2. Seebens, H.; Bacher, S.; Blackburn, T.M.; Capinha, C.; Dawson, W.; Dullinger, S.; Genovesi, P.; Hulme, P.E.; Kleunen, M.V.; Kühn, I.; et al. Projecting the continental accumulation of alien species through to 2050. *Glob. Change Biol.* **2021**, *27*, 970–982. [CrossRef] [PubMed]
3. Vilà, M.; Espinar, J.L.; Hejda, M.; Hejda, M.; Hulme, P.E.; Jarosík, V.; Maron, J.L.; Pergl, J.; Schaffner, U.; Sun, Y.; et al. Ecological impacts of invasive alien plants: A meta-analysis of their effects on species, communities and ecosystems. *Ecol. Lett.* **2011**, *14*, 702–708. [CrossRef] [PubMed]
4. Hulme, P.E. Beyond control: Wider implications for the management of biological invasions. *J. Appl. Ecol.* **2006**, *43*, 835–847. [CrossRef]
5. International Union for Conservation of Nature (IUCN). IUCN Guidelines for the Prevention of Biodiversity Loss due to Biological Invasion. Species, 31, 28–42. Available online: https://portals.iucn.org/library/efiles/documents/Rep-2000-052.pdf (accessed on 27 April 2020).
6. Diagne, C.; Leroy, B.; Vaissière, A.C. High and rising economic costs of biological invasions worldwide. *Nature* **2021**, *592*, 571–576. [CrossRef]
7. Golivets, M.; Wallin, K.F. Neighbour tolerance, not suppression, provides competitive advantage to non-native plants. *Ecol. Lett.* **2018**, *21*, 745–759. [CrossRef]
8. Medvecká, J.; Jarolímek, I.; Hegedüšová, K. Forest habitat invasions—Who with whom, where and why. *For. Ecol. Manag.* **2018**, *409*, 468–478. [CrossRef]
9. Foxcroft, L.C.; Pyšek, P.; Richardson, D.M.; Genovesi, P.; MacFadyen, S. Plant invasion science in protected areas: Progress and priorities. *Biol. Invasions* **2017**, *19*, 1353–1378. [CrossRef]
10. Ministério do Meio Ambiente (MMA). Unidades de Conservação: O Que São. Available online: https://www.mma.gov.br/areas-protegidas/unidades-de-conservação/o-que-sao.html (accessed on 6 May 2020).
11. Ribeiro, M.C.; Metzger, J.P.; Martensen, A.C.; Ponzoni, F.J.; Hirota, M.M. The Brazilian Atlantic Forest: How much is left, and how is the remaining forest distributed? Implications for conservation. *Biol. Conserv.* **2009**, *142*, 1141–1153. [CrossRef]
12. Dechoum, M.S.; Sühs, R.B.; Futada, S.M.; Ziller, S.R. Distribution of Invasive Alien Species in Brazilian Ecoregions and Protected Areas. In *Invasive Alien Species: Observations and Issues from Around the World*, 1st ed.; Pullaiah, T., Ielmini, M.R., Eds.; Wiley: Hoboken, NJ, USA, 2021; Volume 4, pp. 24–42.
13. Stadler, J.; Trefflich, A.; Klotz, S.; Brandl, R. Exotic plant species invade diversity hot spots: The alien flora of northwestern Kenya. *Ecography* **2000**, *23*, 169–176. [CrossRef]
14. Stohlgren, T.J. Beyond theories of plant invasions: Lessons from natural landscapes. *Comments Biol.* **2002**, *7*, 355–379. [CrossRef]
15. Stohlgren, T.J.; Jarnevich, W.E.C.; Morisette, J.T. Bounding Species-Environmental Matching Models. *Curr. Zool.* **2011**, *57*, 642–647. [CrossRef]
16. Foxcroft, L.C.; Richardson, D.M.; Rouget, M.; Macfadyen, S. Patterns of alien plant distribution at multiple spatial scales in a large national park: Implications for ecology, management and monitoring. *Divers. Distrib.* **2009**, *15*, 367–378. [CrossRef]

17. Foxcroft, L.C.; Jarosick, P.P.; Richardson, D.M.; Rouget, M. Protected-Area Boundaries as Filters of Plant Invasions. *Conserv. Biol.* **2011**, *25*, 2. [CrossRef]
18. Didham, R.K.; Tylianakis, J.M.; Hutchison, M.A.; Ewers, R.M.; Gemmell, N.J. Are invasive species the drivers of ecological change? *Trends Ecol. Evol.* **2005**, *20*, 9. [CrossRef]
19. Simberloff, D.; Von Holle, B. Positive interactions of nonindigenous species: Invasional meltdown? *Biol. Inv.* **1999**, *1*, 21–32. [CrossRef]
20. Witt, A.; Beale, T.; Van Wilgen, B.W. An assessment of the distribution and potential ecological impacts of invasive alien plant species in eastern Africa. *Transit. R. Soc. South Afr.* **2018**, *73*, 3. [CrossRef]
21. Allen, J.A.; Brown, C.S.; Stohlgren, T.J. Non-native plant invasions of United States National Parks. *Biol. Invasions* **2009**, *11*, 21–95. [CrossRef]
22. Moodley, D.; Angulo, E.; Cuthbert, R.N.; Leung, B.; Turbelin, A.; Novoa, A.; Kourantidou, M.; Heringer, G.; Haubrock, P.J.; Renault, D.; et al. Surprisingly high economic costs of biological invasions in protected areas. *Biol. Invasions* **2022**, *24*, 1995–2016. [CrossRef]
23. Jacquemoud, S.; Ustin, S. *Leaf Optical Properties*, 1st ed.; Cambridge University Press: Cambridge, UK, 2019; pp. 12–47, 320–556.
24. Serbin, S.P.; Townsend, P.A. Scaling Functional Traits from Leaves to Canopies. In *Remote Sensing of Plant Biodiversity*; Cavender-Bares, J., Gamon, J., Townsend, P., Eds.; Springer: Cham, Switzerland, 2020.
25. Eugenio, F.C.; Schons, C.T.; Mallmann, C.L.; Schuh, M.S.; Fernandes, P.; Badin, T.L. Remotely piloted aircraft systems and forests: A global state of the art and future challenges. *Can. J. For. Research* **2020**, *50*, 705–716. [CrossRef]
26. Papp, L.; van Leeuwen, B.; Szilassi, P.; Tobak, Z.; Szatmári, J.; Árvai, M.; Mészáros, J.; Pásztor, L. Monitoring Invasive Plant Species Using Hyperspectral Remote Sensing Data. *Land* **2021**, *10*, 29. [CrossRef]
27. Gholizadeh, H.; Friedman, M.S.; McMillan, N.A.; Hammond, W.M.; Hassani, K.; Sams, A.V.; Charles, M.D.; Garrett, D.R.; Joshi, O.; Hamilton, R.G.; et al. Mapping invasive alien species in grassland ecosystems using airborne imaging spectroscopy and remotely observable vegetation functional traits. *Remote Sens. Environ.* **2022**, *271*, 112887. [CrossRef]
28. Bolch, E.A.; Santos, M.J.; Ade, C.; Khanna, S.; Basinger, N.T.; Reader, M.O.; Hestir, E.L. Remote Detection of Invasive Alien Species. In *Remote Sensing of Plant Biodiversity*; Cavender-Bares, J., Gamon, J., Townsend, P., Eds.; Springer Nature: Cham, Switzerland, 2020; pp. 267–307. [CrossRef]
29. Khare, S.; Latifi, H.; Ghosh, S.K. Multi-scale assessment of invasive plant species diversity using Pléiades 1A, RapidEye and Landsat-8 data. *Geocarto Int.* **2018**, *33*, 681–698. [CrossRef]
30. Große-Stoltenberg, A.; Hellmann, C.; Thiele, J.; Werner, C.; Oldeland, J. Early detection of GPP-related regime shifts after plant invasion by integrating imaging spectroscopy with airborne LiDAR. *Remote Sens. Environ.* **2018**, *209*, 780–792. [CrossRef]
31. Piiroinena, R.; Fassnacht, F.E.; Heiskanen, J.; Maeda, E.; Mack, B.; Pellikka, P. Invasive tree species detection in the Eastern Arc Mountains biodiversity hotspot using one class classification. *Remote Sens. Environ.* **2018**, *218*, 119–131. [CrossRef]
32. Niphadkar, M.; Nagendra, H. Remote sensing of invasive plants: Incorporating functional traits into the picture. *Int. J. Remote Sens.* **2016**, *37*, 3074–3085. [CrossRef]
33. Diao, C.; Wang, L. Incorporating plant phenological trajectory in exotic saltcedar detection with monthly time series of Landsat imagery. *Remote Sens. Environ.* **2016**, *182*, 60–71. [CrossRef]
34. Rajah, P.; Odindi, J.; Mutanga, O. Evaluating the potential of freely available multispectral remotely sensed imagery in mapping American bramble (*Rubus cuneifolius*). *South Afr. Geogr. J.* **2018**, *100*, 291–307. [CrossRef]
35. Cheng, Y.B.; Tom, E.; Ustin, S.L. Mapping an invasive species, kudzu (*Pueraria montana*), using hyperspectral imagery in western Georgia. *J. Appl. Remote Sens.* **2007**, *1*, 013514. [CrossRef]
36. Brenner, J.C.; Christman, Z.; Rogan, J. Segmentation of Landsat Thematic Mapper Imagery Improves Buffelgrass (Pennisetum Ciliare) Pasture Mapping in the Sonoran Desert of Mexico. *Appl. Geogr.* **2012**, *34*, 569–575. [CrossRef]
37. Hantson, W.; Kooistra, L.; Slim, P.A. Mapping invasive woody species in coastal dunes in the Netherlands: A remote sensing approach using LIDAR and high-resolution aerial photographs. *Appl. Veg. Sci.* **2012**, *15*, 536–547. [CrossRef]
38. Omeer, A.A.; Deshmukh, R.R. Improving the classification of invasive plant species by using continuous wavelet analysis and feature reduction techniques. *Ecol. Inform.* **2021**, *61*, 101181. [CrossRef]
39. Tesfamichael, S.G.; Newete, S.W.; Adam, E.; Byrne, M.J. Discriminating pure Tamarix species and their putative hybrids using field spectrometer. *Geocarto Int.* **2021**, 1–20. [CrossRef]
40. Iqbal, I.M.; Balzter, H.; Shabbir, A. Identifying the Spectral Signatures of Invasive and Native Plant Species in Two Protected Areas of Pakistan through Field Spectroscopy. *Remote Sens.* **2021**, *13*, 4009. [CrossRef]
41. Barbosa, J.M.; Asner, G.P.; Martin, R.E.; Baldeck, C.A.; Hughes, F.; Johnson, T. Determining Subcanopy Psidium cattleianum Invasion in Hawaiian Forests Using Imaging Spectroscopy. *Remote Sens.* **2016**, *8*, 33. [CrossRef]
42. Tesfamichael, S.G.; Newete, S.W.; Adam, E.; Dubula, B. Field spectroradiometer and simulated multispectral bands for discriminating invasive species from morphologically similar cohabitant plants. *GIScience Remote Sens.* **2018**, *55*, 417–436. [CrossRef]
43. Asner, G.P.; Martin, R.E. Spectral and chemical analysis of tropical forests: Scaling from leaf to canopy levels. *Remote Sens. Environ.* **2008**, *112*, 3958–3970. [CrossRef]
44. Resasco, J.; Hale, A.N.; Henry, M.C.; Gorchov, D.L. Detecting an invasive shrub in a deciduous forest understory using late-fall Landsat sensor imagery. *Int. J. Remote Sens.* **2007**, *28*, 3739–3745. [CrossRef]

45. Wilfong, B.N.; Gorchov, D.L.; Henry, M.C. Detecting an invasive shrub in deciduous forest understories using remote sensing. *Weed Sci.* **2009**, *57*, 512–520. [CrossRef]
46. Asner, G.P.; Martin, R.E.K.; Carlson, M.; Rascher, U.; Vitousek, P.M. Vegetation-Climate Interactions among Native and Invasive Species in Hawaiian Rainforest. *Ecosystems* **2006**, *9*, 1106–1117. [CrossRef]
47. Somers, B.; Asner, G.P. Hyperspectral Time Series Analysis of Native and Invasive Species in Hawaiian Rainforests. *Remote Sens.* **2012**, *4*, 2510–2529. [CrossRef]
48. Asner, G.P.; Jones, M.O.; Martin, R.E.; Knapp, D.E.; Hughes, R.F. Remote Sensing of Native and Invasive Species in Hawaiian Forests. *Remote Sens. Environ.* **2008**, *112*, 1912–1926. [CrossRef]
49. Muchoney, D.M. Earth observations for terrestrial biodiversity and ecosystems. *Remote Sens. Environ.* **2008**, *112*, 1909–1911. [CrossRef]
50. Cavender-Bares, J.; Schweiger, A.K.; Pinto-Ledesma, J.N.; Meireles, J.M. Appling Remote Sensing to Biodiversity Science. In *Remote Sensing of Plant Biodiversity*; Cavender-Bares, J., Gamon, J., Townsend, P., Eds.; Springer Nature: Cham, Switzerland, 2020; pp. 13–42. [CrossRef]
51. Schumacher, M.V.; Longhi, S.J.; Brun, E.J.; Kilca, R.V. (Eds.) *A Floresta Estacional Subtropical—Caracterização e Ecologia no Rebordo do Planalto Meridional*; Pallotti: Santa Maria, Brazil, 2011; 320p.
52. Kilca, R.V.; Pedron, F.A.; Schwartz, G.; Longhi, S.J.; Deobald, G.A. Soil changes in a subtropical seasonal forest chronosequences in the south of Brazil. *Ciência Rural* **2015**, *45*, 2174–2180. [CrossRef]
53. Mallmann, C.L.; Prado, D.A.; Pereira Filho, W. Índice de vegetação por diferença normalizada para caracterização da dinâmica florestal no parque estadual Quarta Colônia, estado do Rio Grande do Sul—Brasil. *Rev. Bras. De Geogr. Física* **2015**, *8*, 1–15. [CrossRef]
54. Scipioni, M.C.; Longhi, S.J.; Reinert, D.J.; Araujo, M.M.; Pedron, F.A. Distribuição do compartimento arbóreo em gradiente de relevo e solos na encosta Meridional da Serra Geral, RS. *Ciência Rural* **2010**, *40*, 1295–1301. [CrossRef]
55. Rovedder, A.P.M.; Almeida, C.M.; Araujo, M.M.; Tonetto, T.S.; Scotti, M.S.V. Relação solo-vegetação em remanescente da floresta estacional decidual na Região Central do Rio Grande do Sul. *Ciência Rural* **2014**, *44*, 2178–2185. [CrossRef]
56. Pedron, F.A.; Azevedo, A.C.; Dalmolin, R.S.D.; Stürmer, S.L.K.; Menezes, F.P. Morfologia e Classificação Taxonômica de Neossolos e Saprolitos derivados de rochas vulcânicas da Formação Serra Geral no Rio Grande do Sul. *Rev. Bras. Ciência Solo* **2009**, *33*, 119–128. [CrossRef]
57. Wrege, M.; Steinmetz, S.; Reisser-Junior, C.; Almeida, I. *Atlas Climático da Região Sul do Brasil: Estados do Paraná Santa Catarina e Rio Grande do Sul*; Embrapa Clima Temperado: Pelotas, Brazil; Embrapa Florestas: Colombo, Brazil, 2011.
58. Witt, A.B.R.; Luke, Q. *Guide to the Naturalized and Invasive Plants of Eastern Africa*; CABI: Wallingford, UK, 2017; pp. 416–417. [CrossRef]
59. Carvalho, P.E.R. Ecologia, silvicultura e usos da uva-do-japão (*Hovenia dulcis* Thunberg). Embrapa, 23; CNP-Florestas: Colombo, PR, Brazil, 1994; 24p.
60. Dechoum, M.S.; Castellani, T.T.; Zalba, S.M.; Rejmánek, M.; Peroni, N.; Tamashiro, J.Y. Community structure, succession and invasibility in a seasonal deciduous Forest in southern Brazil. *Biol. Inv.* **2015**, *17*, 1697–1712. [CrossRef]
61. Padilha, L.D.; Loregian, A.C.; Budck, J.C. Forest fragmentation does not matter to invasions by Hovenia dulcis. *Biodivers. Conserv.* **2015**, *24*, 2293–2304. [CrossRef]
62. GBIF Home Page. Available online: https://www.gbif.org (accessed on 1 March 2021).
63. CABI. *Hovenia dulcis* . In *Invasive Species Compendium*; CAB International: Wallingford, UK, 2020; Available online: http://www.cabi.org/isc. (accessed on 26 November 2020).
64. Schorn, L.A.; Meyer, L.; Sevegnani, L.; Vibrans, A.C.; Vanessa, D.; Gasper, L.A.L.; Uhlmman, A.; Verdi, M.; Stival-Santos, A. Fitossociologia de fragmentos de floresta estacional decidual no estado de Santa Catarina—Brasil. *Ciência Florest.* **2014**, *24*, 821–831. [CrossRef]
65. Horus Institute. Horus Institute for Environmental Development and Conservation. Brazilian Invasive Species Database. Available online: http://bd.institutohorus.org.br (accessed on 26 November 2020).
66. Zenni, R.D.; Ziller, S.R. Visão geral das plantas exóticas invasoras no Brasil. *Rev. Bras. Bot.* **2011**, *34*, 431–446. [CrossRef]
67. Schaff, L.; Figueiredo Filho, A.; Galvão, F.; Sanquetta, C.R.; Longhi, S.J. Modificações florístico-estruturais de um remanescente de Floresta Ombrofila Mista Montana no período de 1979 e 2000. *Ciência Florest.* **2006**, *16*, 271–291. [CrossRef]
68. Sitther, V.; Zhang, D.; Harris, D.L. Genetic characterization of guava (*Psidium guajava* L.) germplasm in the United States using microsatellite markers. *Genet. Resour. Crop Evol.* **2014**, *61*, 829–839. [CrossRef]
69. Tuler, A.C.; Carrijo, T.T.; Ferreira, M.F.S.; Peixoto, A.L. Flora of Espírito Santo: Psidium (Myrtaceae). *Rodriguésia* **2017**, *68*, 1791–1805. [CrossRef]
70. Cronk, Q.C.B.; Fuller, J.L. *Plant Invaders: The Threat to Natural Ecosystems*; Chapman & Hall: London, UK, 1995; pp. 127–129. [CrossRef]
71. Smith, C.W. *Pest Plants of Hawaiian Native Ecosystems*; Department of Botany, University of Hawaii: Honolulu, HI, USA, 1998.
72. Weber, E. *Invasive Plant Species of the World: A Reference Guide to Environmental Weeds*; CAB International: Wallingford, UK, 2003.
73. Henderson, L. Alien Weeds and Invasive Plants. In *Plant Protection Research Institute*; Handbook, n 12; Paarl Printers: Cape Town, South Africa, 2001; p. 193.

74. Chapla, T.E.; Campos, J.B. Allelopathic evidence in exotic guava (*Psidium guajava* L.). *Braz. Arch. Biol. Technol.* **2010**, *53*, 1359–1362. [CrossRef]
75. Hiscox, J.D.; Israelstam, G.F. A Method for Extraction of Chlorophyll from Leaf Tissue without Maceration. *Can. J. Botany* **1979**, *57*, 1332–1334. [CrossRef]
76. Lichtenthaler, H.K. Chlorophylls and Carotenoids - pigments of photosynthetic biomembranes. *Methods Enzymol.* **1987**, *148*, 350–382. [CrossRef]
77. Ogashawara, I.; Curtarelli, M.P.; Souza, A.F.; Augusto-Silva, P.B.; Alcântara, E.H.; Stech, J.L. Interactive Correlation Environment (ICE) - A Statistical Web Tool for Data Collinearity Analysis. *Remote Sens.* **2014**, *6*, 3059–3074. [CrossRef]
78. Hill, J.; Buddenbaum, H.; Townsend, P.A. Imaging Spectroscopy of Forest Ecosystems: Perspectives for the Use of Space-borne Hyperspectral Earth Observation Systems. *Surv. Geophys.* **2019**, *40*, 553–588. [CrossRef]
79. Murrins Misiukas, J.; Carter, S.; Herold, M. Tropical Forest Monitoring: Challenges and Recent Progress in Research. *Remote Sens.* **2021**, *13*, 2252. [CrossRef]
80. Ustin, S.L.; Jacquemoud, S. How the Optical Properties of Leaves Modify the Absorption and Scattering of Energy and Enhance Leaf Functionality. In *Remote Sensing of Plant Biodiversity*; Cavender-Bares, J., Gamon, J., Townsend, P., Eds.; Springer Nature: Cham, Switzerland, 2020; pp. 349–384.
81. Danson, F.M.; Bowyer, P. Estimating live fuel moisture content from remotely sensed reflectance. *Remote Sens. Environ.* **2004**, *92*, 309–321. [CrossRef]
82. Riaño, D.; Vaughan, P.; Chuvieco, E.; Zarco-Tejada, P.J.; Ustin, S.L. Estimation of fuel moisture content by inversion of radiative transfer models to simulate equivalent water thickness and dry matter content: Analysis at leaf and canopy level. *IEEE Trans. Geosci. Remote Sens.* **2005**, *43*, 819–826. [CrossRef]
83. Wang, X.; Wotton, B.M.; Cantin, A.S.; Parisien, M.A.; Anderson, K.; Moore, B.; Flannigan, M.D. CFFDRS: An R package for the Canadian forest fire danger rating system. *Ecol. Process.* **2017**, *6*, 5–16. [CrossRef]
84. Yebra, M.; Quanc, X.; Riaño, D.; Larraondo, P.R.; van Dijik, A.I.J.M.; Cary, G.J. A fuel moisture content and flammability monitoring methodology for continental Australia based on optical remote sensing. *Remote Sens. Environ.* **2018**, *212*, 260–272. [CrossRef]
85. Streher, A.S.; Torres, R.S.; Morellato, L.P.C.; Silva, T.S.F. Accuracy and limitations for spectroscopic prediction of leaf traits in seasonally dry tropical environments. *Remote Sens. Environ.* **2020**, *244*, 1118–1128. [CrossRef]
86. Féret, J.B.; Le Maire, G.; Jay, S.; Berveiller, D.; Bendoula, R.; Hmimina, G.; Cheraiet, A.; Oliveira, J.C.; Ponzoni, F.J.; Solanki, T.; et al. Estimating leaf mass per area and equivalent water thickness based on leaf optical properties: Potential and limitations of physical modeling and machine learning. *Remote Sens. Environ.* **2018**, *231*, 110959. [CrossRef]
87. Cheng, T.; Rivard, B.; Sánchez-Azofeifa, G.A.; Féret, J.B.; Jacquemoud, S.; Ustin, S.L. Deriving leaf mass per area (LMA) from foliar reflectance across a variety of plant species using continuous wavelet analysis. *J. Photogramm. Remote Sens.* **2014**, *87*, 28–38. [CrossRef]
88. Asner, G.P.; Martin, R.E.; Knapp, D.E.; Tupayachi, R.; Anderson, C.; Carranza, L.; Martinez, P.; Houcheime, M.; Sinca, F.; Weiss, P. Spectroscopy of canopy chemicals in humid tropical forests. *Remote Sens. Environ.* **2011**, *115*, 3587–3598. [CrossRef]
89. Poorter, H.; Niinemets, U.; Poorter, L.; Wright, I.J.; Villar, R. Causes and consequences of variation in leaf mass per area (LMA): A meta-analysis. *New Phytol.* **2009**, *182*, 565–588. [CrossRef]
90. Wright, I.J.; Reich, P.B.; Westoby, M.; Ackerly, D.D.; Baruch, Z.; Bongers, F.; Cavender-Bares, J.; Chapin, T.; Cornelissen, J.H.C.; Diemer, M.; et al. The worldwide leaf economics spectrum. *Nature* **2004**, *428*, 821–827. [CrossRef]
91. Wright, I.J.; Ackerly, D.D.; Bongers, F.; Harms, K.E.; Ibarra-Manriquez, G.; Martinez-Ramos, M.; Mazer, S.J.; Muller-Landau, H.C.; Paz, H.; Pitman, N.C.A.; et al. Relationships among ecologically important dimensions of plant trait variation in seven neotropical forests. *Ann. Bot.* **2007**, *99*, 1003–1015. [CrossRef]
92. Hoffmann, W.A.; Franco, A.C.; Moreira, M.Z.; Haridasan, M. Specific leaf area explains differences in leaf traits between congeneric savanna and forest trees. *Funct. Ecol.* **2005**, *19*, 932–940. [CrossRef]
93. Bucci, S.J.; Scholz, F.G.; Goldstein, G.; Meinzer, F.C.; Franco, A.C.; Campanello, P.I.; Villalobos-Vega, R.; Bustamante, M.; Miralles-Wilhelm, F. Nutrient availability constrains the hydraulic architecture and water relations of savannah trees. *Plant Cell Environ.* **2006**, *29*, 2153–2167. [CrossRef]
94. Ball, A.; Sanchez-Azofeifa, A.; Portillo Quintero, C.; Rivard, B.; Castro-Contreras, S.; Fernandes, G. Patterns of Leaf Biochemical and Structural Properties of Cerrado Life Forms: Implications for Remote Sensing. *PLoS ONE* **2015**, *10*, e0117659. [CrossRef]
95. Gitelson, A.A.; Merzlyak, M.N.; Chivkunova, O.B. Optical properties and nondestructive estimation of anthocyanin content in plant leaves. *Photochem. Photobiol.* **2001**, *74*, 38–45. [CrossRef]
96. Noomen, M.F.; Skidmore, A.K.; Van Der Meer, F.D.; Prins, H.H.T. Continuum removed band depth analysis for detecting the effects of natural gas, methane and ethane on maize reflectance. *Remote Sens. Environ.* **2006**, *105*, 262–270. [CrossRef]
97. Solovchenko, A. *Photoprotection in Plants Optical Screening-Based Mechanisms*; Springer: Berlin/Heidelberg, Germany, 2010; pp. 89–159.
98. Harrison, D.; Rivard, B.; Sánchez-Azofeifa, A. Classification of tree species based on longwave hyperspectral data from leaves, a case study for a tropical dry forest. *Int. J. Appl. Earth Obs. Geoinf.* **2018**, *66*, 93–105. [CrossRef]
99. Gamon, J.A.; Somers, B.; Malenovský, Z.; Middleton, E.M.; Rascher, U.; Schaepman, M.E. Assessing vegetation function with imaging spectroscopy. *Surv. Geophys.* **2019**, *40*, 489–513. [CrossRef]

100. Le Maire, G.; Francois, C.; Soudani, K.; Berveiller, D.; Pontailler, J.Y.; Bréda, N.; Genet, H.; Davi, H.; Dufrêne, E. Calibration and validation of hyperspectral indices for the estimation of broadleaved forest leaf chlorophyll content, leaf mass per area, leaf area index and leaf canopy biomass. *Remote Sens. Environ.* **2008**, *112*, 3846–3864. [CrossRef]
101. Penuelas, J.; Filella, I.; Biel, C.; Serrano, L.; Savé, R. The reflectance at the 950–970 nm region as an indicator of plant water status. *Int. J. Remote Sens.* **1993**, *14*, 1887–1905. [CrossRef]
102. Gitelson, A. Towards a generic approach to remote non-invasive estimation of foliar carotenoid-to-chlorophyll ratio. *J. Plant Physiol.* **2020**, *252*, 153227. [CrossRef] [PubMed]
103. Danson, F.M.; Steven, M.D.; Malthus, T.J.; Clark, J.A. High-spectral resolution data for determining leaf water content. *Int. J. Remote Sens.* **1992**, *13*, 461–470. [CrossRef]
104. Kumar, L. High-spectral resolution data for determining leaf water content in Eucalyptus species: Leaf level experiments. *Geocarto Int.* **2007**, *22*, 3–16. [CrossRef]